

# Combined $^{18}\text{F}$ -Fluoride and $^{18}\text{F}$ -FDG PET/CT Scanning for Evaluation of Malignancy: Results of an International Multicenter Trial

Andrei Iagaru<sup>1</sup>, Erik Mittra<sup>1</sup>, Camila Mosci<sup>1</sup>, David W. Dick<sup>1</sup>, Mike Sathekege<sup>2</sup>, Vineet Prakash<sup>3</sup>, Victor Iyer<sup>3</sup>, Paula Lapa<sup>4</sup>, Jorge Isidoro<sup>4</sup>, Joao M. de Lima<sup>4</sup>, and Sanjiv Sam Gambhir<sup>5</sup>

<sup>1</sup>Stanford University Medical Center, Stanford, California; <sup>2</sup>Pretoria University Hospital, Pretoria, South Africa; <sup>3</sup>Aalborg University Hospital, Aalborg, Denmark; <sup>4</sup>Serviço de Medicina Nuclear, Hospitais da Universidade de Coimbra, Coimbra, Portugal; and <sup>5</sup>Departments of Radiology, Bioengineering, Materials Science, and Engineering, Molecular Imaging Program at Stanford (MIPS), Stanford University School of Medicine, Stanford, California

$^{18}\text{F}$ -FDG PET/CT is used in a variety of cancers, but because of variable rates of glucose metabolism, not all cancers are reliably identified.  $^{18}\text{F}$ - PET/CT allows for the acquisition of highly sensitive and specific images of the skeleton. We prospectively evaluated combined  $^{18}\text{F}$ -/ $^{18}\text{F}$ -FDG as a single PET/CT examination for evaluation of cancer patients and compared it with separate  $^{18}\text{F}$ - PET/CT and  $^{18}\text{F}$ -FDG PET/CT scans. **Methods:** One hundred fifteen participants with cancer were prospectively enrolled in an international multicenter trial evaluating  $^{18}\text{F}$ - PET/CT,  $^{18}\text{F}$ -FDG PET/CT, and combined  $^{18}\text{F}$ -/ $^{18}\text{F}$ -FDG PET/CT. The 3 PET/CT scans were performed sequentially within 4 wk of one another for each patient. **Results:**  $^{18}\text{F}$ -/ $^{18}\text{F}$ -FDG PET/CT allowed for accurate interpretation of radiotracer uptake outside the skeleton, with findings similar to those of  $^{18}\text{F}$ -FDG PET/CT. In 19 participants, skeletal disease was more extensive on  $^{18}\text{F}$ - PET/CT and  $^{18}\text{F}$ -/ $^{18}\text{F}$ -FDG PET/CT than on  $^{18}\text{F}$ -FDG PET/CT. In another 29 participants,  $^{18}\text{F}$ - PET/CT and  $^{18}\text{F}$ -/ $^{18}\text{F}$ -FDG PET/CT showed osseous metastases where  $^{18}\text{F}$ -FDG PET/CT was negative. The extent of skeletal lesions was similar in 18 participants on all 3 scans. **Conclusion:** This trial demonstrated that combined  $^{18}\text{F}$ -/ $^{18}\text{F}$ -FDG PET/CT shows promising results when compared with separate  $^{18}\text{F}$ - PET/CT and  $^{18}\text{F}$ -FDG PET/CT for evaluation of cancer patients. This result opens the possibility for improved patient care and reduction in health-care costs, as will be further evaluated in future trials.

**Key Words:**  $^{18}\text{F}$ -;  $^{18}\text{F}$ -FDG; PET/CT; cancer

**J Nucl Med 2013; 54:176–183**

DOI: 10.2967/jnumed.112.108803

**P**ET and PET/CT performed with  $^{18}\text{F}$ -FDG is used in a variety of cancers, for which it has changed the practice

Received May 21, 2012; revision accepted Aug. 30, 2012.

For correspondence or reprints contact: Andrei Iagaru, Division of Nuclear Medicine, Stanford University Medical Center, 300 Pasteur Dr., Room H-0101, Stanford, CA 94305.

E-mail: aiagaru@stanford.edu

Published online Dec. 14, 2012

COPYRIGHT © 2013 by the Society of Nuclear Medicine and Molecular Imaging, Inc.

of oncology (1). However, because of variable rates of glucose metabolism, not all malignant lesions are reliably identified, contributing to the overall limitations of this method (2). The initial staging of patients diagnosed with certain cancers includes imaging with  $^{18}\text{F}$ -FDG PET/CT and  $^{99\text{m}}\text{Tc}$ -methylene diphosphonate ( $^{99\text{m}}\text{Tc}$ -MDP) bone scintigraphy as separate studies (3,4).  $^{99\text{m}}\text{Tc}$ -MDP bone scintigraphy is the method of choice for evaluation of osseous metastases, since it allows a whole-body survey at a relatively low cost. Before the introduction of  $^{99\text{m}}\text{Tc}$ -based agents, bone scintigraphy with sodium fluoride-18 ( $^{18}\text{F}$ -) was performed using  $\gamma$ -cameras, despite the fact that 511-keV photons are suboptimal for conventional nuclear medicine scanners (5).  $^{18}\text{F}$ - is a positron emitter; therefore, imaging the skeleton with  $^{18}\text{F}$ -NaF PET/CT allows for the acquisition of highly sensitive and specific images (6). High-quality images of the skeleton can be obtained starting less than 1 h after the intravenous administration of  $^{18}\text{F}$ - (7). The Society of Nuclear Medicine and Molecular Imaging published practice guidelines for  $^{18}\text{F}$ - PET/CT (8), and the Centers for Medicare and Medicaid Services approved reimbursement of  $^{18}\text{F}$ - PET/CT when performed through the National Oncologic PET Registry.

After completing a pilot study on 14 participants (9), we reported the feasibility of combining  $^{18}\text{F}$ - and  $^{18}\text{F}$ -FDG in a single PET/CT scan for cancer detection. We now present the results of a prospective international multicenter study that further investigated combined  $^{18}\text{F}$ -/ $^{18}\text{F}$ -FDG PET/CT for evaluation of the extent of malignancy.

## MATERIALS AND METHODS

The Institutional Review Boards of the 4 participating institutions (Aalborg University [Denmark], Coimbra University [Portugal], Pretoria University [South Africa], and Stanford University [United States]) approved this study. One hundred fifteen consecutive participants (including 14 from the pilot study) were recruited prospectively from November 2007 to July 2012. All participants (63 men and 52 women; age range, 19–84 y; average age  $\pm$  SD, 58.5  $\pm$  14.3 y) gave written informed consent before

enrollment in the trial. All cancer types were included in the study in order to simulate actual clinical experience. Seventeen percent of the participants were referred to determine the initial treatment strategy (formerly diagnosis and initial staging), whereas 83% of the patients were referred for determining a subsequent treatment strategy (including treatment monitoring, restaging, and detection of suspected recurrence). This classification is based on the National Coverage Determination for  $^{18}\text{F}$ -FDG PET for Oncologic Conditions from the Centers for Medicare and Medicaid Services (10). The diagnoses included prostate cancer (41 participants), breast cancer (39 participants), sarcoma (22 participants), and other cancers (13 participants). The participants' clinical data are summarized in Tables 1 and 2. All participants underwent  $^{18}\text{F}$ -PET/CT,  $^{18}\text{F}$ -FDG PET/CT, and combined  $^{18}\text{F}$ -/ $^{18}\text{F}$ -FDG PET/CT. The interval between the first and third scans ranged from 3 to 28 d (average,  $6.7 \pm 4.9$  d).

### PET/CT Protocols and Image Reconstruction

Whole-body images were obtained using the following PET/CT scanners: Discovery LS 600 and 690 (GE Healthcare; Stanford), Discovery VCT (GE Healthcare; Aalborg), Discovery ST (GE Healthcare; Coimbra), and Biograph 40 (Siemens; Pretoria). The patients fasted at least 6 h before the  $^{18}\text{F}$ -FDG scans (separate or combined), and blood glucose levels were less than 150 mg/dL at the time of the  $^{18}\text{F}$ -FDG injection. Approximately 60 min after intravenous administration of the radiopharmaceutical, a multislice helical noncontrast CT scan was obtained from the skull vertex to the toes. This scan was used for attenuation correction and anatomic localization of the administered radiopharmaceuticals. Immediately after the CT scan, an emission PET scan was acquired over the same anatomic regions. The PET images were corrected using segmented attenuation data from the CT scan. PET images were reconstructed with a standard iterative algorithm; reformatted into axial, coronal, and sagittal views; and reviewed centrally (Stanford). The prescribed doses were 370–555 MBq (10–15 mCi)

for  $^{18}\text{F}$ -FDG, 185–370 MBq (5–10 mCi) for  $^{18}\text{F}$ <sup>-</sup>, and 555 MBq (15 mCi) of  $^{18}\text{F}$ -FDG + 185 MBq (5 mCi) of  $^{18}\text{F}$ <sup>-</sup> for the combined scan. For the  $^{18}\text{F}$ <sup>-</sup>/ $^{18}\text{F}$ -FDG scans, the 2 radiotracers were delivered from the local cyclotron facilities in separate syringes and administered sequentially, with less than a minute delay. The order of administration was not controlled.

### Image Analysis

The  $^{18}\text{F}$ <sup>-</sup> PET/CT,  $^{18}\text{F}$ -FDG PET/CT, and  $^{18}\text{F}$ <sup>-</sup>/ $^{18}\text{F}$ -FDG PET/CT images were interpreted in randomized order by 2 board-certified nuclear medicine physicians unaware of the diagnosis and the results of other imaging studies, using the software provided by the manufacturer (Xeleris; GE Healthcare). The readers were masked to the 2 other scans when reading 1 scan in a given patient in order to avoid recall bias. Discrepancies were resolved by a consensus reading. A direct comparison for each detected lesion was performed among the 3 scans. For image interpretation, visual analysis was used instead of quantitative analysis. For  $^{18}\text{F}$ <sup>-</sup> PET/CT, areas of focally increased  $^{18}\text{F}$ <sup>-</sup> skeletal uptake were read as malignant unless a benign etiology for this uptake was identified at the same location on the corresponding CT images. For  $^{18}\text{F}$ -FDG PET/CT, focal  $^{18}\text{F}$ -FDG uptake less than that of the mediastinal blood pool was considered benign, uptake equal to that of the mediastinal blood pool was considered uncertain, and uptake greater than that of the mediastinal blood pool was considered malignant. Prior work has shown the validity of qualitative assessment of  $^{18}\text{F}$ -FDG uptake in various malignancies (11–15). For the  $^{18}\text{F}$ <sup>-</sup>/ $^{18}\text{F}$ -FDG PET/CT scans, the above-mentioned criteria were combined to define focal uptake as benign, uncertain, or malignant.

In the subgroup of participants with more skeletal lesions detected on  $^{18}\text{F}$ <sup>-</sup> PET/CT and combined  $^{18}\text{F}$ <sup>-</sup>/ $^{18}\text{F}$ -FDG PET/CT than on  $^{18}\text{F}$ -FDG PET/CT, CT images of the bones were also evaluated independently by 2 board-certified radiologists masked to the diagnosis and the results of the PET scanning. Discrepancies were resolved by a consensus reading.

Each patient had all 3 scans acquired on the same scanner to avoid variability. Phantom studies were not conducted to calibrate the scanners used at the 4 participating institutions. However, because no quantitative or semiquantitative analyses were used, lack of calibration did not interfere with the results of the study.

### RESULTS

The injected doses of  $^{18}\text{F}$ -FDG ranged from 358.9 to 684.5 (9.7–18.5 mCi) (average,  $503.2 \pm 92.5$  MBq [ $13.6 \pm 2.5$  mCi]) for the separate scans and from 162.8 to 662.3 MBq (4.4–17.9 mCi) (average,  $444 \pm 88.8$  MBq [ $12.0 \pm 2.4$  mCi]) for the combined scans ( $P = 0.0007$ ). The injected doses of  $^{18}\text{F}$ <sup>-</sup> ranged from 144.3 to 503.2 MBq (3.9–13.6 mCi) (average,  $251.6 \pm 96.2$  MBq [ $6.8 \pm 2.6$  mCi]) for the separate scans and from 136.9 to 518 MBq (3.7–14 mCi) (average,  $196.1 \pm 51.8$  MBq [ $5.3 \pm 1.4$  mCi]) for the combined scans ( $P = 0.0001$ ). The time from intravenous administration of the radiopharmaceuticals to imaging ranged from 43 to 157 min (average,  $81.1 \pm 20.2$ ) for the separate  $^{18}\text{F}$ -FDG scans, from 39 to 154 min (average,  $84.5 \pm 23.7$ ) for the separate  $^{18}\text{F}$ <sup>-</sup> scans, and from 52 to 213 min (average,  $86.0 \pm 26.5$ ) for the combined scans. These time differences were not statistically significant. The variations in doses and times from injection to imag-

**TABLE 1**

Clinical Data of Patient Population Included in This Study

Characteristic	Male	Female
<i>N</i>	63	52
Mean age $\pm$ SD (y)	$60.2 \pm 15.4$	$55.7 \pm 13.6$
Stage		
I	2	1
II	21	20
III	21	5
IV	19	26
Initial treatment strategy	10	9
Subsequent treatment strategy	53	43
Primary tumor		
Prostate	41	0
Breast	0	39
Sarcoma	13	9
Lung	2	1
Bladder	2	0
Colon/rectum	2	0
Cervix	0	1
Kidney	1	1
Non-Hodgkin lymphoma	1	0
Larynx	0	1
Paraganglioma	1	0

**TABLE 2**  
Clinical Data of Participants for Whom  $^{18}\text{F}^-$  PET/CT and Combined  $^{18}\text{F}^-/^{18}\text{F}$ -FDG PET/CT Resulted in More Lesions Detected Than Did  $^{18}\text{F}$ -FDG PET/CT

Characteristic	$^{18}\text{F}^-/^{18}\text{F}$ -PET/CT showed more lesions than $^{18}\text{F}^-$ PET/CT	$^{18}\text{F}^-/^{18}\text{F}$ -PET/CT showed lesions; $^{18}\text{F}$ -FDG PET/CT was negative
Male	9	21
Female	10	8
Initial treatment strategy	4	4
Subsequent treatment strategy	15	25
Stage		
I	0	1
II	1	10
III	4	12
IV	14	6
Primary tumor		
Prostate	5	18
Breast	8	5
Sarcoma	4	1
Colon	1	0
Lung	1	0
Bladder	0	1
Kidney	0	2
Larynx	0	1
Cervix	0	1
Prior treatment		
Surgery	1	4
Chemotherapy	1	1
Radiotherapy	0	4
Surgery/chemotherapy	4	4
Surgery/radiotherapy	0	5
Chemotherapy/radiotherapy	4	5
Surgery/chemotherapy/radiotherapy	5	2
None	4	4

Data are numbers of patients.

ing are part of routine clinical practice even at major academic centers (16).

For the 96 patients referred for imaging as part of the subsequent treatment strategy, the time from the most recent treatment to the first scan done as part of the research protocol ranged from 1.5 to 204 mo (average, 44.4 mo).

Combining the findings of the separate  $^{18}\text{F}^-$  PET/CT and  $^{18}\text{F}$ -FDG PET/CT scans resulted in identification of malignant lesions in 82 of the 115 participants. One patient diagnosed with prostate cancer had a pelvic osseous bone metastasis seen on  $^{18}\text{F}$ -FDG PET/CT but not on  $^{18}\text{F}^-$  PET/CT.  $^{18}\text{F}^-$  PET/CT identified bone metastases in 67 of the 115 participants, whereas  $^{18}\text{F}$ -FDG PET/CT detected bone metastases in 38 of the 115 participants. A typical example in Figure 1, of a 74-y-old man with recently diagnosed prostate cancer, shows extensive pelvic osseous metastases seen on the  $^{18}\text{F}^-$  and combined PET scans but not on  $^{18}\text{F}$ -FDG PET. However,  $^{18}\text{F}$ -FDG PET/CT detected extraosseous malignant lesions in 48 of the 115 participants. Figure 2 illustrates extensive extraosseous metastases

seen on the  $^{18}\text{F}$ -FDG and combined scans in a 45-y-old woman with breast cancer. The most common extraskeletal sites of metastases were lymph nodes (28/115 participants), lungs (14/115 participants), and liver (8/115 participants).  $^{18}\text{F}^-/^{18}\text{F}$ -FDG PET/CT missed three  $^{18}\text{F}$ -FDG-avid lung nodules in 2 participants and two  $^{18}\text{F}^-$ -avid skull lesions in another 2 participants. These 4 participants had other sites of disease that were clearly identified on both the individual tracer scans and the combined scans; thus, the missed lesions would not have affected the overall staging.

#### Evaluation of $^{18}\text{F}^-/^{18}\text{F}$ -FDG PET/CT Versus $^{18}\text{F}^-$ PET/CT

Two skull lesions seen on  $^{18}\text{F}^-$  scans were missed on the corresponding  $^{18}\text{F}^-/^{18}\text{F}$ -FDG combined scans. These missed lesions did not change the participants' management, because other skeletal lesions were identified and altered the staging accordingly. The 2 missed skull lesions are presented in Figure 3.

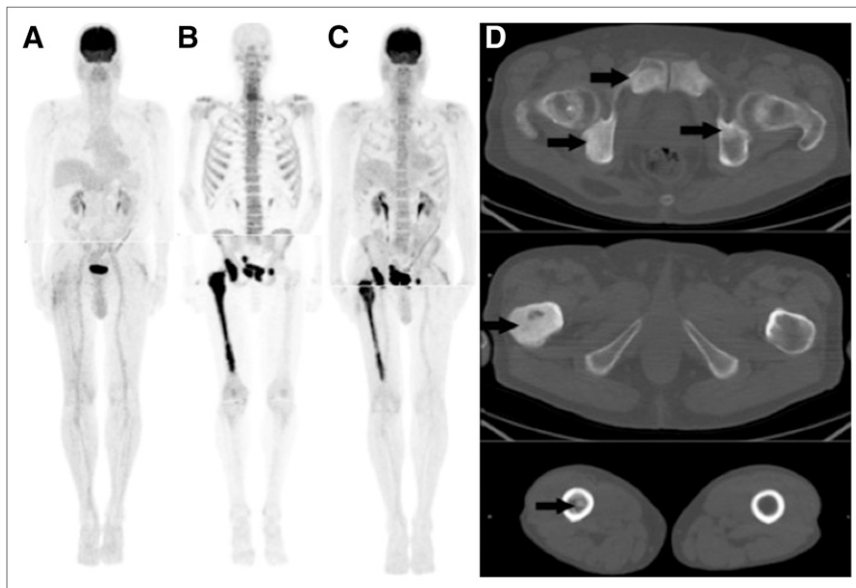


**FIGURE 1.** A 74-y-old man with metastatic prostate cancer. (A–C) Extensive pelvic osseous metastases (arrows) are not identified on  $^{18}\text{F}$ -FDG PET scan (A) but are clearly seen on  $^{18}\text{F}$ - (B) and combined PET (C) scans. (D) CT demonstrates sclerotic changes.

#### Evaluation of $^{18}\text{F}$ -/ $^{18}\text{F}$ -FDG PET/CT Versus $^{18}\text{F}$ -FDG PET/CT

Visual analysis showed that  $^{18}\text{F}$ -/ $^{18}\text{F}$ -FDG PET images allow for accurate interpretation of uptake in the soft tissues. However, small pulmonary nodules were missed in 2 participants. These nodules, less visible on the combined scan than on the  $^{18}\text{F}$ -FDG scan, are shown in Figure 4.

#### Evaluation of $^{18}\text{F}$ - PET/CT Versus $^{18}\text{F}$ -FDG PET/CT

In 19 participants, skeletal metastases were more extensive on  $^{18}\text{F}$ - PET/CT and combined  $^{18}\text{F}$ -/ $^{18}\text{F}$ -FDG PET/CT than on  $^{18}\text{F}$ -FDG PET/CT. When CT data were analyzed alone, bone metastases were identified in 17 patients, fewer lesions than on the PET data were seen in 1 patient, and findings were negative despite lesions seen on PET in 1 patient. In 29 participants,  $^{18}\text{F}$ - PET/CT showed osseous

metastases not present on  $^{18}\text{F}$ -FDG PET/CT. In this subgroup, CT alone identified bone metastases in 15 patients, whereas fewer lesions than on the PET data were seen in 8 patients and CT was negative despite lesions seen on PET in 6 patients. The extent of osseous metastases was similar in another 18 patients on all 3 scans. In 1 participant,  $^{18}\text{F}$ -FDG PET/CT showed focal radiopharmaceutical uptake in a lytic skeletal metastasis not identified prospectively on  $^{18}\text{F}$ - PET/CT. In retrospect, a rim of increased  $^{18}\text{F}$ - uptake was noted around this lesion. The remaining 47 (of 115 total) patients had no osseous metastases identified on any of the 3 scans.

#### DISCUSSION

Published data support the use of bone imaging ( $^{99\text{m}}\text{Tc}$ -MDP or  $^{18}\text{F}$ -) and  $^{18}\text{F}$ -FDG PET/CT for detection of skeletal

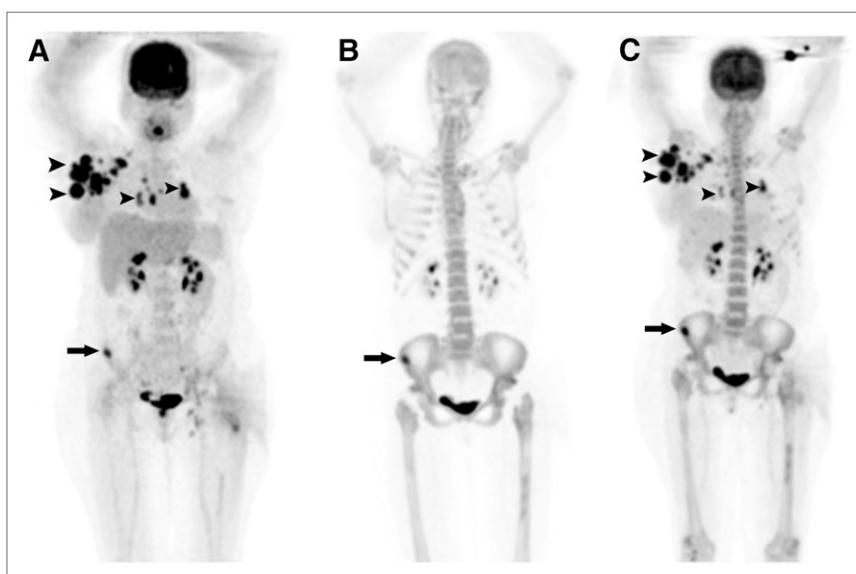


**FIGURE 2.** A 45-y-old woman with metastatic breast cancer. Extensive soft-tissue metastases (arrowheads) are seen on  $^{18}\text{F}$ -FDG (A) and combined PET (C) scans. A single bone metastasis (arrow) is visualized on all 3 scans.

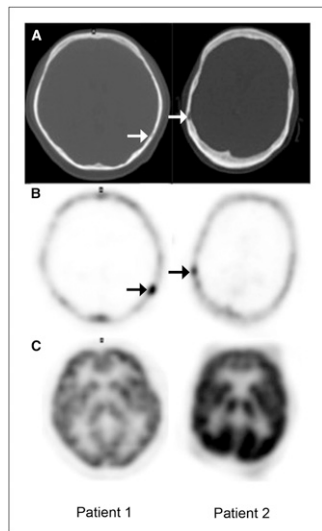


**FIGURE 3.** Skull lesions (arrows) are identified in 2 participants on CT (A) and  $^{18}\text{F}^-$  PET (B) scans but not on combined  $^{18}\text{F}^-$  scans (C).

metastases in selected cancer patients, as both lytic and sclerotic lesions may coexist and have different mechanisms of radiotracer uptake. The spatial resolution of  $^{99\text{m}}\text{Tc}$ -MDP planar scintigraphy and SPECT affects their sensitivity for detection of osseous metastases. Thus, the transition to the better resolution of PET/CT for detection of osseous metastases appears appealing, with  $^{18}\text{F}^-$  as the radiotracer of choice.  $^{18}\text{F}^-$  PET/CT is superior to  $^{99\text{m}}\text{Tc}$ -MDP planar scintigraphy and SPECT for bone lesion detection (17–20). Semiquantitative analysis based on  $^{18}\text{F}^-$  PET/CT is also more accurate than  $^{99\text{m}}\text{Tc}$ -MDP SPECT for assessing the response to treatment of bone metastases (21).

$^{18}\text{F}$ -FDG PET/CT provides unique information on the glucose metabolism of certain skeletal lesions (22). The location of a metastasis in the skeleton and the aggressiveness of the tumor itself are important with regard to the extent of the metabolic response induced and therefore the amount of  $^{18}\text{F}$ -FDG uptake (23). Published data suggest that  $^{18}\text{F}$ -FDG PET is less sensitive than bone scintigraphy for prostate cancer in the detection of osseous metastatic lesions but may be useful in the detection of metastatic nodal and soft-tissue disease (24,25). Other investigators have shown that the level of  $^{18}\text{F}$ -FDG uptake in prostate cancer lesions is an independent prognostic factor and provides complementary prognostic information to  $^{99\text{m}}\text{Tc}$ -MDP bone scans (26).

The use of both  $^{18}\text{F}^-$  PET/CT and  $^{18}\text{F}$ -FDG PET/CT may be needed in patients with selected cancers. In this study we combined 2 separate scans into a single imaging procedure, providing evidence of the superiority of this approach, which may be cost-effective and convenient for selected cancer patients. Before the advent of combined PET/CT technology, Hoegerle et al. reported the use of combined  $^{18}\text{F}^-$ / $^{18}\text{F}$ -FDG administration for PET (27). Indeed, the authors attempted to use skeletal  $^{18}\text{F}^-$  uptake as a surrogate for anatomic localization of abnormal  $^{18}\text{F}$ -FDG in the absence of fused PET and CT. In their study, the images obtained after combined administration were not compared with separate  $^{18}\text{F}^-$  and  $^{18}\text{F}$ -FDG scans in every participant. With the availability of PET/CT, an entirely new combined radiotracer approach allows for a strategy for patient management not previously possible.

Skull lesions seen on  $^{18}\text{F}^-$  PET and subcentimeter-sized lung nodules seen on  $^{18}\text{F}$ -FDG PET were missed on the combined scan in 4 participants. One missed skull lesion was from a combined scan acquired at 213 min after injection of 170.2 MBq (4.6 mCi) of  $^{18}\text{F}^-$  and 488.4 MBq (13.2 mCi) of  $^{18}\text{F}$ -FDG. Therefore it is conceivable that the delayed time to imaging may have contributed to the non-visualization. The proximity to the rib cage of the lung nodules less visible on the combined scan than on the separate  $^{18}\text{F}$ -FDG scan and the  $^{18}\text{F}^-$  uptake in the osseous structures may have contributed to this lack of clear identification. However, none of these missed lesions changed the participants' management, because other lesions were identified. We anticipate that future research optimizing the ratio of  $^{18}\text{F}^-$  to  $^{18}\text{F}$ -FDG dosages in the combined scan may solve the infrequent issue of less well visualized lesions on the combined scan than on the separate scans. In fact, recent data suggest that a ratio of 1:5 may be optimal when  $^{18}\text{F}^-$  and  $^{18}\text{F}$ -FDG are administered for the cocktail approach (27). We are also exploring image reconstruction strategies that will minimize the chance of such missed lesions on the combined scan.

We acknowledge that some of the lesions that were identified on the combined scans due to the addition of  $^{18}\text{F}^-$  may represent treatment-related changes (i.e., bone repair) and not active metastases, as our patient population included patients already treated. However, additional lesions were also found in patients presenting for initial staging. Although this may represent a limitation of the study, our

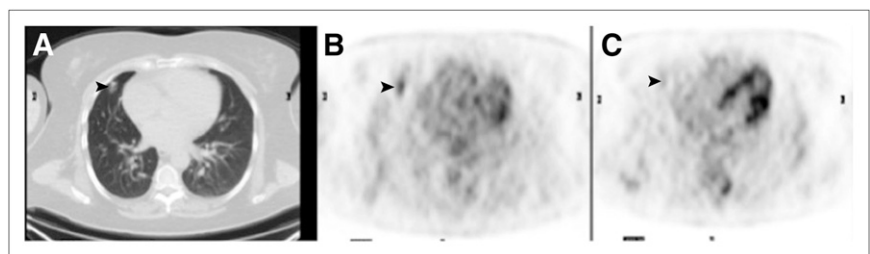


**FIGURE 4.** A 53-y-old woman with soft-tissue sarcoma. Lung nodule (arrowheads) is seen on CT (A) and  $^{18}\text{F}$ -FDG PET (B) scans but is not easily identifiable on combined  $^{18}\text{F}^-$ / $^{18}\text{F}$ -FDG scans (C).

**TABLE 3**  
Limitations and Issues Identified in this Trial, as Well as Potential Solutions to Investigate Them

Issue	Potential solution
Ratio of $^{18}\text{F}^-$ and $^{18}\text{F}$ -FDG dosages	Conduct dose modeling or phantom studies to determine optimal ratio of $^{18}\text{F}^-$ to $^{18}\text{F}$ -FDG for combined scan
Sensitivity and specificity of $^{18}\text{F}^-$ / $^{18}\text{F}$ -FDG PET/CT	Conduct prospective trials with pathology or follow-up evaluation of detected lesions
Quantitation of radiotracer uptake	Conduct experiments to determine influence of $^{18}\text{F}^-$ uptake on $^{18}\text{F}$ -FDG maximum standardized uptake value and vice versa
Interpretation of follow-up studies	Conduct prospective studies to evaluate feasibility or usefulness of $^{18}\text{F}^-$ / $^{18}\text{F}$ -FDG PET/CT in posttherapy setting
$^{18}\text{F}^-$ nonspecific uptake	Analyze CT data to increase specificity

goal was to demonstrate that  $^{18}\text{F}^-$ / $^{18}\text{F}$ -FDG PET/CT shows promising results, not to document the performance of CT or separate  $^{18}\text{F}$ -FDG PET or  $^{18}\text{F}^-$  PET for detection of true-positive malignant lesions. Therefore, we did not assess the identified lesions as true-positive, true-negative, false-positive, or false-negative at the central-site reading. This issue will be further evaluated in future research.

Other limitations of this study included the participants' heterogeneous cancer types, the selection bias toward patients with known malignancy, and the different disease stages of the participants. To come to statistically sound conclusions regarding the appropriate indications for  $^{18}\text{F}^-$ / $^{18}\text{F}$ -FDG PET/CT, further prospective enrollment of subjects is needed, focusing on particular cancer groups. Furthermore, bone marrow-stimulating therapy induces intense  $^{18}\text{F}$ -FDG uptake in the skeleton (29) and may play a confounding role in the evaluation of osseous structures on  $^{18}\text{F}^-$ / $^{18}\text{F}$ -FDG PET. This particular instance of evaluation of response to therapy by  $^{18}\text{F}^-$ / $^{18}\text{F}$ -FDG PET/CT also needs to be separately evaluated in future studies. Another limitation of the study is that semiquantitative analysis of the radiopharmaceutical uptake such as standardized uptake value measurements was not performed. Semiquantitative analysis of  $^{18}\text{F}^-$  PET/CT scans is still an evolving field that has no standardized procedures and lacks validation (8). Issues such as the effect of  $^{18}\text{F}^-$  on bone and soft-tissue uptake of  $^{18}\text{F}$ -FDG when given simultaneously also have not been explored. An analysis of these issues

was beyond the scope of the current study. Although this kind of analysis should certainly be addressed in future evaluations, the conclusions on the feasibility of combined  $^{18}\text{F}^-$ / $^{18}\text{F}$ -FDG scans drawn from this study remain valid. The limitations and issues identified in this trial, as well as potential solutions to investigate them, are listed in Table 3.

With regard to radiation exposure,  $^{99\text{m}}\text{Tc}$ -MDP bone scintigraphy results in approximately 4.2 mSv (420 mrem) and  $^{18}\text{F}$ -FDG PET/CT in approximately 26.5 mSv (2,650 mrem) (1.1 mSv/MBq [110 mrem/mCi] from  $^{18}\text{F}$ -FDG and 10 mSv [1,000 mrem] from low-dose CT), or a total of 30.7 mSv (3,070 mrem). Combining  $^{18}\text{F}^-$  PET/CT and  $^{18}\text{F}$ -FDG PET/CT in a single examination will result in a total of 31.5 mSv (3,150 mrem) (1.1 mSv/MBq [110 mrem/mCi] from  $^{18}\text{F}$ -FDG, 1.0 mSv/MBq [100 mrem/mCi] from  $^{18}\text{F}^-$ , and 10.0 mSv [1,000 mrem] from low-dose CT). Using these estimates and the range and average of injected doses, the participants in the study received 10.67–20.35 mSv (1,067–2,035 mrem) (average, 15.18–2.75 mSv [1,518 ± 275 mrem]) from the separate  $^{18}\text{F}$ -FDG scans, 3.90–13.60 mSv (390–1,360 mrem) (average, 6.90–2.60 mSv [690 ± 260 mrem]) from the separate  $^{18}\text{F}^-$  scans, and 4.84–19.69 mSv (484–1,969 mrem) (average, 13.31 ± 2.64 mSv [1,331 ± 264 mrem]) from  $^{18}\text{F}$ -FDG and 3.70–14.00 mSv (370–1,400 mrem) (average, 15.18 ± 2.75 mSv [1,518 ± 275 mrem]) from  $^{18}\text{F}^-$  in the combined scans. The newest PET/CT scanners have increased sensitivity, and the doses of  $^{18}\text{F}$ -FDG and  $^{18}\text{F}^-$  can be reduced further (30), result-

**TABLE 4**  
Cost Estimates for Separate  $^{99\text{m}}\text{Tc}$ -MDP Bone Scan and  $^{18}\text{F}$ -FDG PET/CT vs. Combined  $^{18}\text{F}^-$ / $^{18}\text{F}$ -FDG PET/CT Scan

$^{99\text{m}}\text{Tc}$ -MDP bone scan	$^{18}\text{F}$ -FDG PET/CT	$^{18}\text{F}^-$ / $^{18}\text{F}$ -FDG PET/CT
Technical reimbursement: \$275	Technical reimbursement: \$1,421	Technical reimbursement: \$1,421
Professional reimbursement: \$48	Professional reimbursement: \$140	Professional reimbursement: \$140
$^{99\text{m}}\text{Tc}$ -MDP: \$100	$^{18}\text{F}$ -FDG: \$250	$^{18}\text{F}$ -FDG: \$250
Total: \$423	Total: \$1,811	$^{18}\text{F}^-$ : \$150
Total: \$2,234		Total: \$1,961

ing in less radiation exposure from  $^{18}\text{F}$ -/ $^{18}\text{F}$ -FDG PET/CT. Thus, instead of patients having to get a separate  $^{99\text{m}}\text{Tc}$ -MDP bone scan or  $^{18}\text{F}$ -FDG PET/CT study, usually on different days, our strategy allows for a single combined PET/CT scan with potentially more utility, lower radiation dose, and greater patient convenience. The recent introduction of hybrid PET/MR technology in clinical practice (31–33) may lead to the use of the combined approach with PET/MR scanners in specific indications, resulting in even less radiation exposure.

Using the current reimbursement rate from the Centers for Medicare and Medicaid Services, we estimate that approximately \$273 in reimbursement may be saved per patient by performing  $^{18}\text{F}$ -/ $^{18}\text{F}$ -FDG PET/CT instead of separate  $^{18}\text{F}$ -FDG PET/CT and  $^{99\text{m}}\text{Tc}$ -MDP bone scintigraphy. Not everyone referred for these imaging procedures will be a candidate for the combined scan. However, considering that approximately 2 million  $^{99\text{m}}\text{Tc}$ -MDP bone scans are performed annually to evaluate malignancy in the United States, and assuming that approximately 500,000  $^{18}\text{F}$ -FDG PET/CT scans are performed in the same population, the combined scan can potentially amount to a total of approximately \$136.5 million saved annually in reimbursement (Table 4). Therefore, this strategy may allow for potentially significant cost savings for the health-care system. Although these estimates may be representative of the health-care costs in the United States, the actual savings in the health-care systems of the other participating centers is unknown.

## CONCLUSION

This prospective multicenter trial indicated promising results for  $^{18}\text{F}$ -/ $^{18}\text{F}$ -FDG PET/CT when compared with separate  $^{18}\text{F}$ - PET/CT and  $^{18}\text{F}$ -FDG PET/CT in the evaluation of cancer patients. This finding opens the possibility for improved patient care and reduction of health-care costs. Further evaluation of this proposed imaging modality is warranted to identify the most suitable scenarios for routine clinical use.

## DISCLOSURE

The costs of publication of this article were defrayed in part by the payment of page charges. Therefore, and solely to indicate this fact, this article is hereby marked “advertisement” in accordance with 18 USC section 1734. This research was supported in part by NCI ICMIC CA114747, and the clinical studies were supported in part by the Doris Duke Foundation and NECSA/NTP. No other potential conflict of interest relevant to this article was reported.

## ACKNOWLEDGMENTS

We thank Drs. Srihari Sampath and Srinath Sampath for assistance with the interpretation of CT images of the bones,

all the technologists at the participating sites, our research fellow Khun Visith Keu, our clinical research coordinators Lindee Burton and Euodia Jonathan, and Dr. Frederick Chin in the Cyclotron Facility, as well as all the participants and their families. The ClinicalTrials.gov identifier for this study is NCT00725387.

## REFERENCES

- Hillner BE, Siegel BA, Liu D, et al. Impact of positron emission tomography/computed tomography and positron emission tomography (PET) alone on expected management of patients with cancer: initial results from the national oncologic PET registry. *J Clin Oncol*. 2008;26:2155–2161.
- Kapoor V, McCook BM, Torok FS. An introduction to PET-CT imaging. *Radiographics*. 2004;24:523–543.
- Podoloff DA, Ball D, Ben-Josef E, et al. NCCN task force: clinical utility of PET in a variety of tumor types. *J Natl Compr Canc Netw*. 2009;7(suppl 2):S1–S26.
- Savelli G, Maffioli L, Maccauro M, De Deckere E, Bombardieri E. Bone scintigraphy and the added value of SPECT (single photon emission tomography) in detecting skeletal lesions. *Q J Nucl Med*. 2001;45:27–37.
- Shirazi PH, Rayudu GV, Fordham EW. Review of solitary  $^{18}\text{F}$  bone scan lesions. *Radiology*. 1974;112:369–372.
- Even-Sapir E, Metser U, Flusser G, et al. Assessment of malignant skeletal disease: initial experience with  $^{18}\text{F}$ -fluoride PET/CT and comparison between  $^{18}\text{F}$ -fluoride PET and  $^{18}\text{F}$ -fluoride PET/CT. *J Nucl Med*. 2004;45:272–278.
- Grant FD, Fahey FH, Packard AB, et al. Skeletal PET with  $^{18}\text{F}$ -fluoride: applying new technology to an old tracer. *J Nucl Med*. 2008;49:68–78.
- Segall G, Delbeke D, Stabin MG, et al. SNM practice guideline for sodium  $^{18}\text{F}$ -fluoride PET/CT bone scans 1.0. *J Nucl Med*. 2010;51:1813–1820.
- Iagaru A, Mitra E, Yaghoubi SS, et al. Novel strategy for a cocktail  $^{18}\text{F}$ -fluoride and  $^{18}\text{F}$ -FDG PET/CT scan for evaluation of malignancy: results of the pilot-phase study. *J Nucl Med*. 2009;50:501–505.
- Kitajima K, Suzuki K, Nakamoto Y, et al. Low-dose non-enhanced CT versus full-dose contrast-enhanced CT in integrated PET/CT studies for the diagnosis of uterine cancer recurrence. *Eur J Nucl Med Mol Imaging*. 2010;37:1490–1498.
- Shamim SA, Kumar R, Shandal V, et al. FDG PET/CT evaluation of treatment response in patients with recurrent colorectal cancer. *Clin Nucl Med*. 2011;36:11–16.
- Onishi Y, Ohno Y, Koyama H, et al. Non-small cell carcinoma: comparison of postoperative intra- and extrathoracic recurrence assessment capability of qualitatively and/or quantitatively assessed FDG-PET/CT and standard radiological examinations. *Eur J Radiol*. 2011;79:473–479.
- Schmidt M, Schmalenbach M, Jungehlsing M, et al.  $^{18}\text{F}$ -FDG PET for detecting recurrent head and neck cancer, local lymph node involvement and distant metastases: comparison of qualitative visual and semiquantitative analysis. *Nuklearmedizin*. 2004;43:91–101.
- Gallowitsch H-J, Kresnik E, Gasser J, et al. F-18 fluorodeoxyglucose positron-emission tomography in the diagnosis of tumor recurrence and metastases in the follow-up of patients with breast carcinoma: a comparison to conventional imaging. *Invest Radiol*. 2003;38:250–256.
- Juweid ME, Stroobants S, Hoekstra OS, et al. Use of positron emission tomography for response assessment of lymphoma: consensus of the Imaging Subcommittee of International Harmonization Project in Lymphoma. *J Clin Oncol*. 2007;25:571–578.
- Graham MM, Badawi RD, Wahl RL. Variations in PET/CT methodology for oncologic imaging at U.S. academic medical centers: an imaging response assessment team survey. *J Nucl Med*. 2011;52:311–317.
- Even-Sapir E, Metser U, Mishani E, et al. The detection of bone metastases in patients with high-risk prostate cancer:  $^{99\text{m}}\text{Tc}$ -MDP planar bone scintigraphy, single- and multi-field-of-view SPECT,  $^{18}\text{F}$ -fluoride PET, and  $^{18}\text{F}$ -fluoride PET/CT. *J Nucl Med*. 2006;47:287–297.
- Ben-Haim S, Israel O. Breast cancer: role of SPECT and PET in imaging bone metastases. *Semin Nucl Med*. 2009;39:408–415.
- Iagaru A, Mitra E, Dick DW, Gambhir SS. Prospective evaluation of  $^{99\text{m}}\text{Tc}$ -MDP scintigraphy,  $^{18}\text{F}$  NaF PET/CT, and  $^{18}\text{F}$  FDG PET/CT for detection of skeletal metastases. *Mol Imaging Biol*. 2012;14:252–259.

20. Withofs N, Grayet B, Tancredi T, et al.  $^{18}\text{F}$ -fluoride PET/CT for assessing bone involvement in prostate and breast cancers. *Nucl Med Commun.* 2011;32:168–176.
21. Cook G, Parker C, Chua S, et al.  $^{18}\text{F}$ -fluoride PET: changes in uptake as a method to assess response in bone metastases from castrate-resistant prostate cancer patients treated with  $^{223}\text{Ra}$ -chloride (Alpharadin). *EJNMMI Research.* 2011;1:4.
22. Feldman F, van Heertum R, Manos C.  $^{18}\text{F}$ FDG PET scanning of benign and malignant musculoskeletal lesions. *Skeletal Radiol.* 2003;32:201–208.
23. Fogelman I, Cook G, Israel O, Van der Wall H. Positron emission tomography and bone metastases. *Semin Nucl Med.* 2005;35:135–142.
24. Jadvar H, Pinski J, Conti P. FDG PET in suspected recurrent and metastatic prostate cancer. *Oncol Rep.* 2003;10:1485–1488.
25. Shiiba M, Ishihara K, Kimura G, et al. Evaluation of primary prostate cancer using  $^{11}\text{C}$ -methionine-PET/CT and  $^{18}\text{F}$ -FDG-PET/CT. *Ann Nucl Med.* 2012;26:138–145.
26. Meirelles GSP, Schöder H, Ravizzini GC, et al. Prognostic value of baseline [ $^{18}\text{F}$ ] fluorodeoxyglucose positron emission tomography and  $^{99\text{m}}\text{Tc}$ -MDP bone scan in progressing metastatic prostate cancer. *Clin Cancer Res.* 2010;16:6093–6099.
27. Hoegerle S, Juengling F, Otte A, et al. Combined FDG and [ $^{18}\text{F}$ ]fluoride whole-body PET: a feasible two-in-one approach to cancer imaging? *Radiology.* 1998;209:253–258.
28. Richmond K, McLean N, Rold T, et al. Optimizing a F-18 NaF and FDG cocktail as a preclinical cancer screening tool for molecular imaging. *J Nucl Med.* 2011;52(suppl):517P.
29. Kazama T, Swanston N, Podoloff D, Macapinlac H. Effect of colony-stimulating factor and conventional- or high-dose chemotherapy on FDG uptake in bone marrow. *Eur J Nucl Med Mol Imaging.* 2005;32:1406–1411.
30. Surti S, Scheuermann J, El Fakhri G, et al. Impact of time-of-flight PET on whole-body oncologic studies: a human observer lesion detection and localization study. *J Nucl Med.* 2011;52:712–719.
31. Pichler BJ, Judenhofer M, Wehrl H. PET/MRI hybrid imaging: devices and initial results. *Eur Radiol.* 2008;18:1077–1086.
32. Zaidi H, Ojha N, Morich M, et al. Design and performance evaluation of a whole-body Ingenuity TF PET-MRI system. *Phys Med Biol.* 2011;56:3091–3106.
33. Boss A, Bisdas S, Kolb A, et al. Hybrid PET/MRI of intracranial masses: initial experiences and comparison to PET/CT. *J Nucl Med.* 2010;51:1198–1205.





The Journal of  
NUCLEAR MEDICINE

## Combined $^{18}\text{F}$ -Fluoride and $^{18}\text{F}$ -FDG PET/CT Scanning for Evaluation of Malignancy: Results of an International Multicenter Trial

Andrei Iagaru, Erik Mittra, Camila Mosci, David W. Dick, Mike Sathekge, Vineet Prakash, Victor Iyer, Paula Lapa, Jorge Isidoro, Joao M. de Lima and Sanjiv Sam Gambhir

*J Nucl Med.* 2013;54:176-183.

Published online: December 14, 2012.

Doi: 10.2967/jnumed.112.108803

---

This article and updated information are available at:

<http://jnm.snmjournals.org/content/54/2/176>

---

Information about reproducing figures, tables, or other portions of this article can be found online at:

<http://jnm.snmjournals.org/site/misc/permission.xhtml>

Information about subscriptions to JNM can be found at:

<http://jnm.snmjournals.org/site/subscriptions/online.xhtml>

*The Journal of Nuclear Medicine* is published monthly.  
SNMMI | Society of Nuclear Medicine and Molecular Imaging  
1850 Samuel Morse Drive, Reston, VA 20190.  
(Print ISSN: 0161-5505, Online ISSN: 2159-662X)

© Copyright 2013 SNMMI; all rights reserved.